DOE/ID/12778-2
(DE92016808)

HIGH TEMPERATURE CATALYTIC MEMBRANE REACTORS

Topical Report

March 1990

Work Performed Under Contract No. FC07-88ID12778

For
U.S. Department of Energy
Office of Industrial Technologies
Washington, D.C.

By
Alcoa
Warrendale, Pennsylvania

DISCLAIMER

This report was prepared as an account of work sponsored by an agency of the United States Government. Neither the United States Government nor any agency thereof, nor any of their employees, makes any warranty, express or implied, or assumes any legal liability or responsibility for the accuracy, completeness, or usefulness of any information, apparatus, product, or process disclosed, or represents that its use would not infringe privately owned rights. Reference herein to any specific commercial product, process, or service by trade name, trademark, manufacturer, or otherwise does not necessarily constitute or imply its endorsement, recommendation, or favoring by the United States Government or any agency thereof. The views and opinions of authors expressed herein do not necessarily state or reflect those of the United States Government or any agency thereof.

This report has been reproduced directly from the best available copy.

Available to DOE and DOE contractors from the Office of Scientific and Technical Information, P.O. Box 62, Oak Ridge, TN 37831; prices available from (615)576-8401.

Available to the public from the National Technical Information Service, U. S. Department of Commerce, 5285 Port Royal Rd., Springfield, VA 22161.

Printed in the United States of America, Office of Scientific and Technical Information, Oak Ridge , Tennessee

DOE/ID/12778--2

DE92 016808

HIGH TEMPERATURE CATALYTIC MEMBRANE REACTORS

Topical Report

March 1990

Work Performed Under Contract No. DE-FC07-88ID12778

Prepared for the
U.S. Department of Energy
Under DOE Idaho Field Office
Sponsored by the Office of the Assistant Secretary
for Conservation and Renewable Energy
Office of Industrial Technologies
Washington, D.C.

Prepared by
Alcoa
Separations Technology Division
181 Thorn Hill Road
Warrendale, Pennsylvania 15086

Table of Content

List of Tables and Figures

1. Abstract of Program

Current state-of-the-art inorganic oxide membranes offer the potential of being modified to yield catalytic properties. The resulting modules may be configured to simultaneously induce catalytic reactions with product concentration and separation in a single processing step. Processes utilizing such catalytically active membrane reactors have the potential for dramatically increasing yield of reactions which are currently limited by either thermodynamic equilibria, product inhibition, or kinetic selectivity. Examples of commercial interest include hydrogenation, dehydrogenation, partial and selective oxidation, hydrations, hydrocarbon cracking, olefin metathesis, hydroformylation, and olefin polymerization. A large portion of the most significant reactions fall into the category of high temperature, gas phase chemical and petrochemical processes. Microporous oxide membranes are well suited for these applications.

A program is proposed to investigate selected model reactions of commercial interest (i.e. dehydrogenation of ethylbenzene to styrene and dehydrogenation of butane to butadiene) using a high temperature catalytic membrane reactor. Membranes will be developed, reaction dynamics characterized, and production processes developed, culminating in laboratory-scale demonstration of technical and economic feasibility.

As a result, the anticipated increased yield per reactor pass economic incentives are envisioned. First, a large decrease in the temperature required to obtain high yield should be possible because of the reduced driving force requirement. Significantly higher conversion per pass implies a reduced recycle ratio, as well as reduced reactor size. Both factors result in reduced capital costs, as well as savings in cost of reactants and energy. Moreover, the controlled, defined reaction zone (the membrane interface), will facilitate the reactor design process and permit greater control of reactor dynamics, including mass and heat transfer (both of which will now be convective, rather than conductive) should result in more efficient reactor control and design. Lower reactor temperatures also imply possibly less stringent catalyst requirements, as well as the potential to carry out reactions directly that were previously multi-step. Because of the innumerable reactions of commercial interest in the chemical process industries fall into these categories, commercial impact could be enormous.

2. Technical Highlights

The reaction system of ethylbenzene dehydrogenation was modified to improve its hardware flexibility and accuracy. The modified system reproduced the previous results operated at the same reaction conditions using I-Fe_2O_3-2 (2.03 wt% iron oxide/alumina) catalyst. In addition, material balance was performed for the experimental results obtained thus far. The differences in carbon and hydrogen balances between feed and discharges range from 0.51 to 3.19% indicating the experimental results reported from this operating system are reliable.

A comprehensive mathematical model is proposed for describing the performance of catalytic membrane reactors using commercially available membranes. This model is capable of simulating various reaction conditions and different reactor configurations, and will be used for optimization, scale-up and engineering study in the future.

3. Ethylbenzene Dehydrogenation to Styrene

In our year I study, we have completed the evaluation of catalytic membrane reactors using commercially available ceramic membranes. We have demonstrated a 15 to 25% conversion increase along with 2 to 5% increase in selectivity using the existing granular catalysts packed in the membrane. The results indicated that the concept of using existing ceramic membrane with granular catalysts is a viable approach for the development of catalytic membrane reactors.

In year II, we plan to continue to pursue the concept along this line, including the use of commercial catalysts, and acquisition of kinetic parameters for modeling. Some effort has been performed to improve the existing hardware system and precision, which are discussed as follows.

3.1 Hardware Modification

The reactor system was modified to improve flexibility and accuracy measurement. Figure 1 shows the modified membrane reactor system for ethylbenzene dehydrogenation. The ethylbenzene saturator was replaced by an HPLC pump because the delivery of ethylbenzene by a saturator previously used was difficult to control. Water and ethylbenzene (liquid phase) were directly and separately fed into the heated stainless steel tube (as an evaporator) at 190°C in a nitrogen stream. Thus, the feeding rates of ethylbenzene and water can be accurately controlled and measured.

Both permeate and reject streams contain saturation levels of moisture even after cooled by the chiller (5°C). In order to get an accurate measurement of flow rate and also to protect the mass flow meter, desiccant cells were placed before mass flow meters.

3.2 Mass Balance Confirmation

After the hardware modifications described above, two additional runs were conducted to verified the accuracy and reproducibility of the previous experiemntal results.

The overall material balance has been performed to verify the accuracy of the experimental results. Tables 1 and 2 list the results of two runs with I-Fe_2O_3-2 catalyst at 600°C and 640°C, and with water to ethylbenzene ratio of 1.26 and 6.74, respectively. The catalyst used contains 2.03 wt% Fe_2O_3 doped with 4.25 wt% K_2O. It was selected for confirmation of material balance although its performance was inferior to the other catalyst, I-Fe_2O_3-4, loaded with 2.87 wt% Fe_2O_3. The differences in carbon and hydrogen balances between feed and discharges range from 0.51 to 3.19% indicating the experimental results reported from this operating system are reliable.

In the Year I study, the conversion reported ranges from 20 to 25% and the selectivity for styrene from 93 to 94% at 600°C, a higher temperature, at

640°C, the conversion was enhanced to 50 to 60% and the selectivity for styrene was reduced to 84 to 88% with I-Fe_2O_3-2 catalyst. Additional two runs with similar operating conditions were performed with the modified system. The conversions and selectivities were listed in Tables 1 and 2 close to the previous results. These experiments confirmed the reproducibility of ethylbenzene dehydrogenation in the membrane reactor.

3.3 Preparation of Additional Fe_2O_3 Catalyst

Our result in Year I study indicates that conversion of ethylbenzene increased along with the increase of iron content from 2.03 to 2.87 wt%. To evaluate the maximum capability of the reactor, another batch of ion-exchanged iron oxide catalyst with a higher iron content was prepared. The preparation method was similar to that of I-Fe_2O_3-4 described in the last report[1]. The characterization data are listed in Table 3 along with those prepared previously. The iron oxide content of these catalysts is about 6-7 wt% probably due to the higher surface area of alumina support which provides more ion-exchange sites. These catalysts with a higher iron content may improve the performance of the catalytic ethylbenzene dehydrogenation in the membrane reactor and will be used for optimization in the future.

4. Mathematical Modeling of Membrane Reactors

4.1 Literature Review

A mathematical model for the membrane reactor has been developed to simulate the performance of the catalytic membrane reactor. It may provide us a broad understanding of catalytic membrane reactors which can be a very costly exercise from the experimental viewpoint. A model can also help us to find optimum reaction conditions since it is time-consuming and sometimes is impossible to vary all reaction conditions in the laboratory. This model is capable of simulating various reaction conditions and different reactor configurations, and will be used for optimization, scale-up, and engineering study in the future.

Mathematical simulation of membrane reactors has been described in the literature[2,3,4,5,6]. They are summarized in Table 4. None of these models can describe a membrane reactor practical for field operation. Backmixing of flow could exist in a membrane reactor, especially in the shell side since there is no catalyst packing. In a dehydrogenation reaction, total pressures in the shell and tube sides will change along the tubular membrane reactor resulting from hydrogen generation.

This mathematical model attempts to describe a general flow pattern in both tube and shell sides through the incorporation of dispersion coefficients. In addition, the local total pressures (both tube and shell sides) are described as a function of the sum of all components. Shell side can be operated with or without inert purge.

4.2 Material Balance

The model is established with the following assumptions:

- Ideal gas.
- Knudsen diffusion without interactions between components.
- Isothermal condition.
- Steady state.
- Controlling mas transfer resistance: residing in the permselective layer.

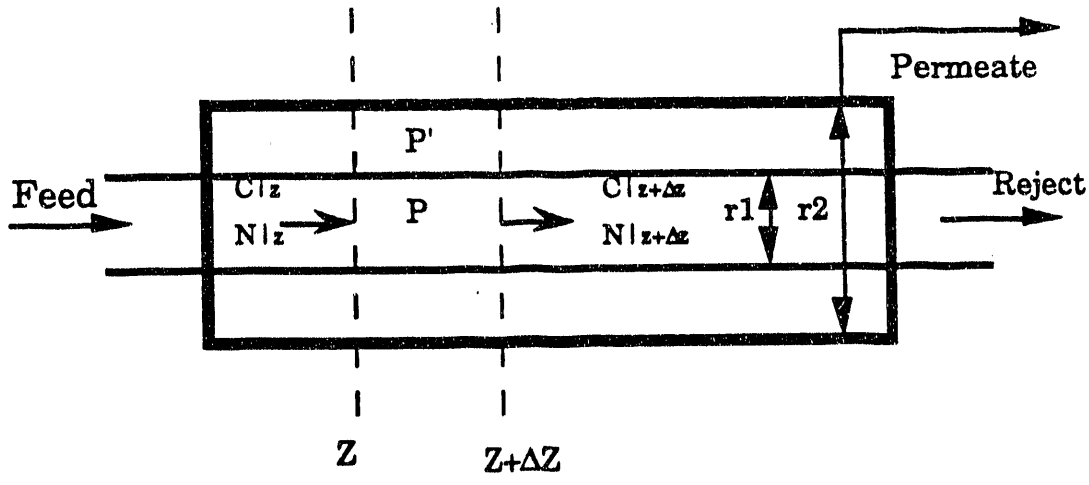

Mass balance for the membrane reactor is described with

Rate of (input - output) = Rate of (permeation + reaction)

The reaction rate is described as follows:

Reaction rate = (Specific rate) x (driving force)

$$\text{Specific rate} = k_0' \cdot \exp(-\frac{E_a}{RT})$$

$$\text{driving force} = (P_i - \frac{P_{i+1} \cdot P_{i+2}}{K_p})$$

Equations for the tube and shell sides are listed as follows:

Tube Side:

$$\pi r_1^2 \cdot [(-D_{1T}\frac{dc_1}{dz}|_z - (-D_{1T}\frac{dc_1}{dz}|_{z+\Delta z})] + \pi r_1^2 \cdot [N_1|_z - N_1|_{z+\Delta z}]$$

$$= 2\pi r_1 \Delta z \cdot K_1 \cdot (P_1 - P_1') + \pi r_1^2 \cdot \Delta z \cdot k'_0 \cdot \exp(-\frac{E_a}{RT}) \cdot (P_1 - \frac{P_2 \cdot P_3}{K_p}) \qquad [1]$$

$$\pi r_1^2 \cdot [(-D_{2T}\frac{dc_2}{dz}|_z - (-D_{2T}\frac{dc_2}{dz}|_{z+\Delta z})] + \pi r_1^2 \cdot [N_2|_z - N_2|_{z+\Delta z}]$$

$$= 2\pi r_1 \Delta z \cdot K_2 \cdot (P_2 - P_2') - \pi r_1^2 \cdot \Delta z \cdot k'_0 \cdot \exp(-\frac{E_a}{RT}) \cdot (P_2 - \frac{P_2 \cdot P_3}{K_p}) \qquad [2]$$

$$\pi r_1^2 \bullet [(-D_{3T}\frac{dc_3}{dz}|_z - (-D_{3T}\frac{dc_3}{dz}|_{z+\Delta z})] + \pi r_1^2 \bullet [N_3|_z - N_3|_{z+\Delta z}]$$

$$= 2\pi r_1 \Delta z \bullet K_3 \bullet (P_3 - P_3') - \pi r_1^2 \bullet \Delta z \bullet k'_0 \bullet \exp(-\frac{E_a}{RT}) \bullet (P_3 - \frac{P_2 \bullet P_3}{K_p}) \quad [3]$$

$$\pi r_1^2 \bullet [(-D_{4T}\frac{dc_4}{dz}|_z - (-D_{4T}\frac{dc_4}{dz}|_{z+\Delta z})] + \pi r_1^2 \bullet [N_4|_z - N_4|_{z+\Delta z}]$$

$$= 2\pi r_1 \Delta z \bullet K_4 \bullet (P_4 - P_4') \quad [4]$$

Shell Side:

$$(\pi r_2^2 - \pi r_1^2) \bullet [(-D_{1S}\frac{dc'_1}{dz}|_z - (-D_{1S}\frac{dc'_1}{dz}|_{z+\Delta z})] +$$

$$(\pi r_2^2 - \pi r_1^2) \bullet [N'_1|_z - N'_1|_{z+\Delta z}] = -2\pi r_1 \Delta z \bullet K_1 \bullet (P_1 - P_1') \quad [5]$$

$$(\pi r_2^2 - \pi r_1^2) \bullet [(-D_{2S}\frac{dc'_2}{dz}|_z - (-D_{2S}\frac{dc'_2}{dz}|_{z+\Delta z})] +$$

$$(\pi r_2^2 - \pi r_1^2) \bullet [N'_2|_z - N'_2|_{z+\Delta z}] = -2\pi r_1 \Delta z \bullet K_2 \bullet (P_2 - P_2') \quad [6]$$

$$(\pi r_2^2 - \pi r_1^2) \bullet [(-D_{3S}\frac{dc'_3}{dz}|_z - (-D_{3S}\frac{dc'_3}{dz}|_{z+\Delta z})] +$$

$$(\pi r_2^2 - \pi r_1^2) \bullet [N'_3|_z - N'_3|_{z+\Delta z}] = -2\pi r_1 \Delta z \bullet K_3 \bullet (P_3 - P_3') \quad [7]$$

$$(\pi r_2^2 - \pi r_1^2) \bullet [(-D_{4S}\frac{dc'_4}{dz}|_z - (-D_{4S}\frac{dc'_4}{dz}|_{z+\Delta z})] +$$

$$(\pi r_2^2 - \pi r_1^2) \bullet [N'_4|_z - N'_4|_{z+\Delta z}] = -2\pi r_1 \Delta z \bullet K_4 \bullet (P_4 - P_4') \quad [8]$$

Where
- i = 1 ethylbenzene
- i = 2 styrene
- i = 3 hydrogen
- i = 4 diluent (water or nitrogen)

Material balance for the diluent (water or nitrogen) is described with equations 4 and 8.

4.3 Mathematical Model Development

When Δz approaches 0,

Tube side:

$$-\frac{D_{1T}}{RT}\bullet\frac{d^2P_1}{dz^2}+\frac{dN_1}{dz}-\frac{2K_1}{r_1}\bullet(P_1-P_1')-k_0\bullet(P_i-\frac{P_2\bullet P_3}{K_p})=0 \qquad [9]$$

$$-\frac{D_{2T}}{RT}\bullet\frac{d^2P_2}{dz^2}+\frac{dN_2}{dz}-\frac{2K_2}{r_1}\bullet(P_2-P_2')+k_0\bullet(P_2-\frac{P_2\bullet P_3}{K_p})=0 \qquad [10]$$

$$-\frac{D_{3T}}{RT}\bullet\frac{d^2P_3}{dz^2}+\frac{dN_3}{dz}-\frac{2K_3}{r_1}\bullet(P_3-P_3')+k_0\bullet(P_3-\frac{P_2\bullet P_3}{K_p})=0 \qquad [11]$$

$$-\frac{D_{4T}}{RT}\bullet\frac{d^2P_4}{dz^2}+\frac{dN_4}{dz}-\frac{2K_4}{r_1}\bullet(P_4-P_4')=0 \qquad [12]$$

Shell side:

$$-\frac{D_{1S}}{RT}\bullet\frac{d^2P_1'}{dz^2}+\frac{dN_1'}{dz}+\frac{2K_1r_1}{r_2^2-r_1^2}\bullet(P_1-P_1')=0 \qquad [13]$$

$$-\frac{D_{2S}}{RT}\bullet\frac{d^2P_2'}{dz^2}+\frac{dN_2'}{dz}+\frac{2K_2r_1}{r_2^2-r_1^2}\bullet(P_2-P_2')=0 \qquad [14]$$

$$-\frac{D_{3S}}{RT}\bullet\frac{d^2P_3'}{dz^2}+\frac{dN_3'}{dz}+\frac{2K_3r_1}{r_2^2-r_1^2}\bullet(P_3-P_3')=0 \qquad [15]$$

$$-\frac{D_{4S}}{RT}\bullet\frac{d^2P_4'}{dz^2}+\frac{dN_4'}{dz}+\frac{2K_4r_1}{r_2^2-r_1^2}\bullet(P_4-P_4')=0 \qquad [16]$$

The relations between partial pressures and molar fluxes are described in equations 17, 18, 19, and 20.

Tube side:

$$P_1 = (\frac{N_1}{\sum N_1}) \bullet P_t \quad [17]$$

$$P_2 = (\frac{N_2}{\sum N_2}) \bullet P_t \quad [18]$$

$$P_3 = (\frac{N_3}{\sum N_3}) \bullet P_t \quad [19]$$

$$P_4 = (\frac{N_4}{\sum N_4}) \bullet P_t \quad [20]$$

Shell side:

$$P_1' = (\frac{N_1'}{\sum N_1'}) \bullet P_t' \quad [21]$$

$$P_2' = (\frac{N_2'}{\sum N_2'}) \bullet P_t' \quad [22]$$

$$P_3' = (\frac{N_3'}{\sum N_3'}) \bullet P_t' \quad [23]$$

$$P_4' = (\frac{N_4'}{\sum N_4'}) \bullet P_t' \quad [24]$$

The local total pressure change along the reactor can be described by:

Tube side:

$$\frac{dP_t}{dz} = \frac{P_t}{\sum N_i} \bullet (\frac{dN_1}{dz} + \frac{dN_2}{dz} + \frac{dN_3}{dz} + \frac{dN_4}{dz}) \quad [25]$$

Shell side:

$$\frac{dP_t'}{dz} = \frac{P_t'}{\sum N_i'} \bullet (\frac{dN_1'}{dz} + \frac{dN_2'}{dz} + \frac{dN_3'}{dz} + \frac{dN_4'}{dz}) \quad [26]$$

The above analysis yields 18 differential equations with 18 dependent variables, i.e.:

Tube side : $N_1, N_2, N_3, N_4, P_1, P_2, P_3, P_4, P_t$

Shell side : N_1', N_2', N_3' , N_4', P_1', P_2' , P_3', P_4', P_t'

and 18 boundary conditions as follows:

$N_1 = N_{10}$ (known value)	at z=0
$N_4 = N_{40}$ (known value)	at z=0
$N_2, N_3 = 0.0$	at z=0
$N_1', N_2', N_3', N_4' = 0.0$	at z=0
$P_1 = P_{10}$ (known value)	at z=0
$P_4 = P_{40}$ (known value)	at z=0
$P_2, P_3 = 0.0$	at z=0
$P_1', P_2', P_3', P_4' = 0.0$	at z=0
$P_t = P_{tL}$ (known value)	at z=L
$P'_t = P'_{tL}$ (known value)	at z=L

where

P_i : tube side pressure (atm)
P_i': shell side pressure (atm)
N_i: molar flux on tube side (mole/m^2/sec)
N_i': molar flux on shell side (mole/m^2/sec)
r_1: inside radius of tube (m)
r_2: inside radius of shell (m)
D_{iT}: tube dispersion coefficient of component i in mixture(m^2/sec)
D_{iS}: shell dispersion coefficient of component i in mixture(m^2/sec)
c_i: tube side concentration (mole/m^3)
c_i': shell side concentration (mole/m^3)
K_i: Knudsen permeability (mole/m^2/atm/sec)
k'_0: rate constant (mole/m^3/atm/sec)
k_0: rate constant at given temperature (mole/m^3/atm/sec)
E_a: activation energy of reaction (Kcal/mole)
K_p: equilibrium constant (atm) $= \frac{P_{H2} \cdot P_{sty}}{P_{eb}}$
P_t: tube side total pressure (atm)
P_t': shell side total pressure (atm)
R: gas constant (cal/mole/K or, atm-m^3/mole/K)

For Knudsen permeability:

$$K_i = \frac{2 \cdot r_3 \cdot \varepsilon_p}{3 \cdot \tau \cdot R \cdot T \cdot L} \cdot \sqrt{8000 \cdot R \cdot \frac{T}{\tau \cdot M_i}} \qquad [27]$$

where

M_i: molecular weight (g/mole)
r_3: pore radius (m)
R: gas constant 8.313 (Pa-m^3/mole/K)
ε_p: porosity
τ: tortuosity
L: thickness of membrane layer (m)

4.4 Future Work

Future work will be focused on the following areas:

- Establish the FORTRAN program
- Simulation study
- Equations of Energy balance
- Engineering analysis and filed application

Table 1

Mass Balance for Ethylbenzene Dehydrogenation in Membrane Reactor
(25 cm, 40Å membrane packed with 8.619 g I-Fe_2O_3 -2 catalyst at 600°C)

Experimental Condition

	Feed	Reject	Permeate
Press.(psig)	2.8	1.1	1.1
Flow Rate Ethylbenzene	4.2381	2.6885	0.5122
Styrene	0.0	0.8645	0.0929
Toluene	0.0	0.0386	0.0081
Benzene	0.0	0.0325	0.0113
Hydrogen	0.0	1.2369	0.1083
Methane	0.0	0.0756	0.0075
CO	0.0	0.0202	0.0048
CO_2	0.0	0.2410	0.0467
H2O	11.1111	11.6670	0.0022
EB/H_2O =	1.26		

Material Balance

Flow Rate (mmole/min)	Feed	Reject	Permeate	% difference
C	33.9048	29.2263	5.0249	1.02
H	64.6032	60.4152	6.2496	3.19

Results

Conversion = 24.5%
Selectivity for styrene = 92.3%

2.2321 mmole/min nitrogen was fed with ethylbenzene.

Table 2

Mass Balance for Ethylbenzene Dehydrogenation in Membrane Reactor
(25 cm, 40Å membrane packed with 8.619 g I-Fe_2O_3-2 catalyst at 640°C)

Experimental Condition

	Feed	Reject	Permeate
Press.(psig)	3.3	1.1	1.8
Flow Rate (mmole/min)			
Ethylbenzene	4.255	1.905	0.352
Styrene	0.0	1.503	0.242
Toluene	0.0	0.087	0.054
Benzene	0.0	0.074	0.050
Hydrogen	0.0	2.460	0.252
Methane	0.0	0.184	0.034
CO	0.0	0.078	0.014
CO_2	0.0	0.542	0.069
H2O	28.667	25.600	2.330
EB/H_2O =	6.74		

Material Balance

Flow rate (mmole/min)	Feed	Reject	Permeate	% difference
C	34.040	29.121	5.407	1.43
H	99.890	89.070	11.328	0.51

Results

Conversion = 47.0%
Selectivity for styrene = 87.0%

2.2321 mmole/min nitrogen was fed with ethylbenzene.

Table 3 :

Characteristics of Iron Oxide/Alumina Catalysts

Sample	Temperature (°C)	K (wt%)	Fe (wt%)	S.A. (M^2/g)	Phase
I-Fe_2O_3-3	800	0.00	3.55	167.7	γ-alumina
I-Fe_2O_3-4	800	5.74	2.87	132.5	γ-alumina
I-Fe_2O_3-5	800	0.00	6.72	168.5	γ-alumina
I-Fe_2O_3-6	800	5.95	6.12	156.4	γ-alumina

Table 4 : Mathematical Modeling of Membrane Reactor

Source	Reactions	Equations	Assumptions	Conclusions
1) Mohan & Govind (ref.3)	Cyclohexane dehydrogenation on Pd-Al_2O_3 or Pt-Al_2O_3 in a membrane reactor.	1.Material balances. 2.Reaction rate is expressed by partial pressures.	1.Isothermal 2.Negligible pressure drop on tube and shell side (isobaric). 3.Plug flows on both tube and shell sides.	1.An optimum ratio of permeation to reaction rate exists for a given length of reactor to achieve a maximum conversion. 2.For a given flow rate and shell/tube pressure ratio, a maximum conversion exists for a reasonable reactor length. 3.A membrane with a high permselectivity for the products should be used in order to achieve a high conversion.
2) Itoh et al. (ref:2)	Cyclohexane dehydrogenation in a vycor-glass membrane reactor	1.Material balances. 2.Reaction rate is expressed by partial pressures.	1.Isothermal. 2.Isobaric 3.Plug flows on tube and shell sides. 4.No axial or radial dispersing. 5.Knudsen diffusion through porous membrane is dominant.	1.Optimum tube thickness for maximum conversion depends on the relative rates of permeation and reaction.
3) Itoh (ref:4)	Cyclohexane dehydrogenation in Pd membrane	1.Material balances. 2. Permeation rate of H_2 obeys the half-power pressure law. 3.Reaction rate is expressed by partial pressures.	1.Isothermal 2.Isobaric 3.Plug flows.	1.100% conversion is expected at high permeate purge or vacuum on the permeate side for a given length of reactor. 2.No separation of the products is need for a complete conversion due to the use of Pd membrane.

Table 4 : Mathematical Modeling of Membrane Reactor (continued)

Source	Reactions	Equations	Assumptions	Conclusions
4) Sun & Khang (ref:5)	Cyclohexane dehydrogenation in vycor glass membrane impregnated with Pt.	1.Material balances. 2.Reaction rate is expressed by partial pressures.	1.Isothermal 2.Mass-transfer resistance in membrane is dominant. 3.Well-mixed in feed and permeate sides.	1.The equilibrium shift effect is significant in high space time operation. 2.The catalytic membrane reactor is superior to the inert membrane packed with catalyst. 3.Strong internal mass-transfer resistance in membrane layer was verified by experiment.
5) Itoh & Govind (ref:6)	Oxidative dehydrogenation of butene to butadiene in a palladium membrane.	1.Material balances. 2.Heat balances 3.Reaction rate is expressed by partial pressures. 4.Permeation rate of H_2 obeys the half-power pressure law.	1.Plug flows in both tube and shell sides 2.No axial or radial diffusion. 3.Insignificant pressure drop along the tube in both sides.	1.Higher conversion can be achieved by hydrogen oxidation on permeate side. 2.Counter-current mode of operation gives a much higher conversion than that of co-current operation.

Figure 1 :
Modified Reaction System for Ethylbenzene Dehydrogenation

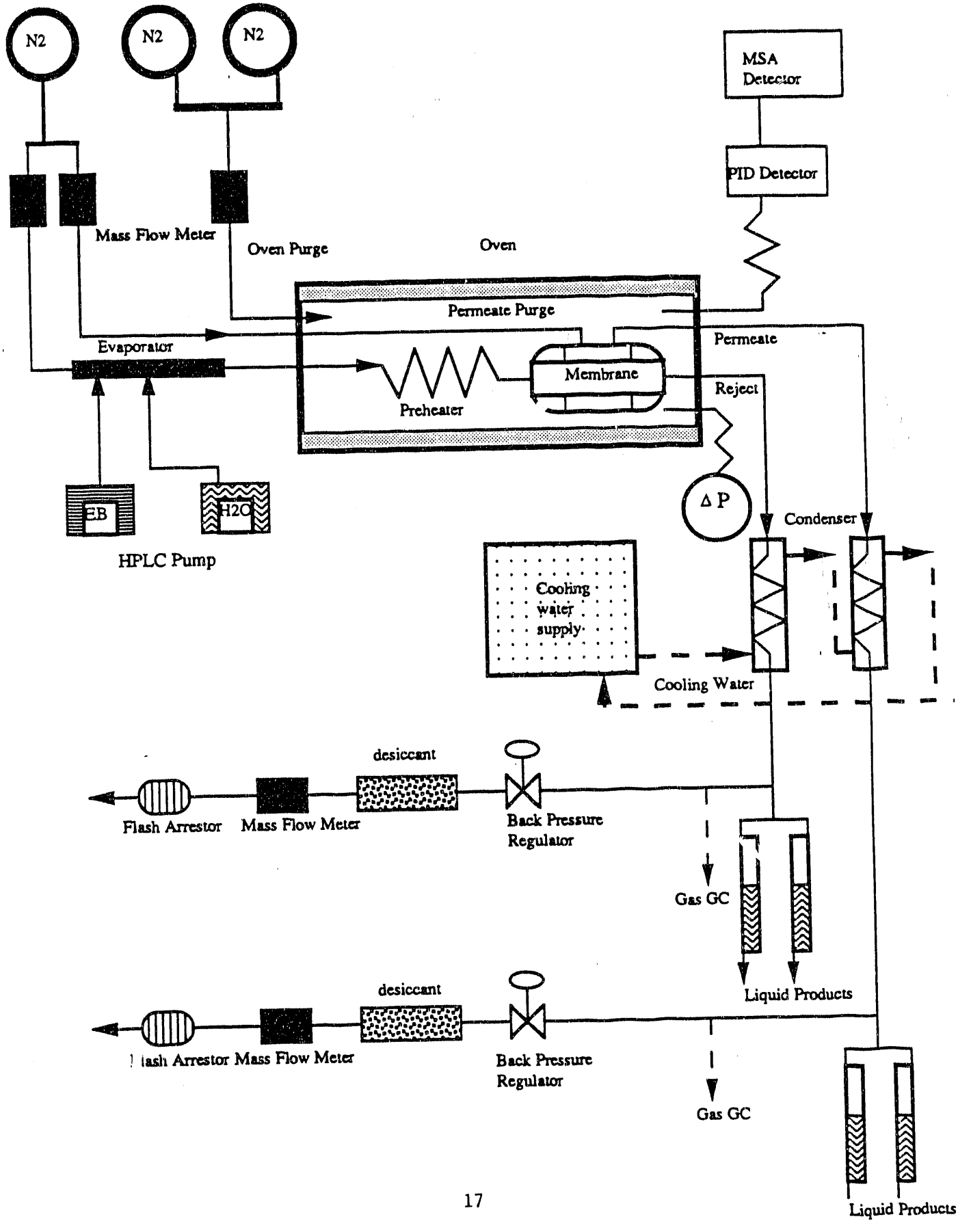

References

1 Wu, J. C.-S., Gerdes, T., Martin, E., Bhave, R. and Liu, P., "Ethylbenzene Dehydrogenation in Microporous Catalytic Membrane Reactors," Progress Report for High Temperature Catalytic Membrane Reactors, DE-FC07-88ID12778, Sept.28 (1989).

2 Itoh, N., Shindo, Y., Haraya, K., Obata, K., Hakuta, T. and Yoshitome, H., "Simulation of A Reaction Accompanied by Separation," International Chemical Engineering, 25(1), p.138 (1985).

3 Mohan, K. and Govind, R., "Analysis of a Cocurrent Membrane Reactor," AIChE Journal, 32(12), p.2083 (1986)

4 Itoh, N., "A Membrane Reactor using Palladium," AIChE Journal, 33(9), p.1576 (1987).

5 Sun, Y.-M. and Khang, S.-J., "Catalytic Membrane for Simultaneous Chemical reaction and Separation Applied to a Dehydrogenation Reaction," Ind. Eng., Chem., Res., 27, 1136 (1988).

6 Itoh, N. and Govind, R., "Development of Novel Oxidative Palladium Membrane Reactor," AIChE Symposium series 268, Vol. 85, 10 (1989).

END

DATE
FILMED
9/01/92